

Effect of Chain Stiffness on Polyelectrolyte Condensation

Malek O. Khan* and Derek Y. C. Chan†

*Particulate Fluids Processing Centre, Department of Mathematics & Statistics, The University of Melbourne, Parkville, Victoria 3010, Australia**Received April 27, 2004; Revised Manuscript Received December 5, 2004*

ABSTRACT: The effect of adding tetravalent counterions to polyelectrolytes of varying stiffness is investigated by a flat histogram Monte Carlo technique that is capable of giving the free energy of the system by direct simulation. The ensemble average of the polyelectrolyte size decreases with the amount of added salt for all chain stiffness. When examining the size distribution functions, flexible chains have narrow end-to-end distance distribution functions for all amounts of added salt. The distribution functions for semiflexible polyelectrolytes are always broader because such chains fluctuate between stretched and collapsed conformations. For stiff chains, the distribution functions show double maxima, which reflect the fact that individual chains prefer to be in elongated or compact toroid conformations, but not inbetween. This coexistence between compact and elongated conformations for stiff polyelectrolytes, when multivalent salt is added, is manifested in force–extension curves which exhibit a plateau regime in which the chain size changes markedly at a constant force.

1. Introduction

Basic understanding of polymers requires characterization of their conformational behavior. An ideal polymer, where no interactions are present between the monomeric units, has a Gaussian size distribution and the average root-mean-square end-to-end distance is given by $R_{ee} = \langle \sqrt{R_{ee}^2} \rangle \simeq b\sqrt{N}$, where N is the number of monomers and b is the length of the bonds separating the monomers.

Interactions between the monomers will affect the conformation of a polymer. Interactions can be of either nonpolymer character or polymer character. Nonpolymer interactions are those for which a monomer will interact with all other monomers, e.g., van der Waals, electrostatic and overlap repulsion. Polymer specific interactions are those that only involve the nearest neighbors along the polymer backbone and affect the bond length and chain stiffness.

It is well-known that a charged polymer (polyelectrolyte) in aqueous solution with only monovalent counterions will adopt an extended conformation in comparison to an uncharged chain.¹ Adding salt to the solution will screen the electrostatic interactions and lead to less extended conformations. This behavior is predicted by mean field theories and simulations in which the electrostatic interactions are modeled by the screened Coulomb potential are capable of reproducing experimental findings.²

Recently it has been observed in simulations in which all Coulombic interactions involving charges on the polyelectrolyte and the small ions are considered explicitly that the predictions of mean field theory or the use of screened Coulomb potentials can be incorrect. In particular, in the limit of strong electrostatic interactions a polyelectrolyte can actually decrease in size.^{3–7} This is thought to be due to counterion correlations which always give an attractive contribution to the effective monomer–monomer interaction. Fluorescence microscopy experiments, involving extremely dilute

DNA solutions, confirm the existence of such single chain condensation phenomena.^{8–10}

Early simulation work^{4–6} was carried out using polyelectrolyte models with flexible backbones, whereas many important molecules are known to be stiff. For example DNA is extremely stiff with a persistence length of about 500 Å. More recent simulation work⁷ and integral equation calculations¹¹ reported a difference in the condensed structure for stiff chains, which are toroid or rodlike, in comparison to the flexible chains, which do not condense to any specific structure. This observation is similar to the variation in collapsing behavior of stiff uncharged polymers, induced by poor solvents.^{12–14} Generally, the persistence length of a polyelectrolyte is decided by short-range interactions and electrostatic interactions. Both can work to either elongate or compact the chain depending on the electrochemical environment. Compaction can be achieved by either poor solvent or strong electrostatics, e.g., when multivalent counterions are present or when the solvent has a small dielectric constant.

For uncharged flexible polymers with solvent mediated intrachain attraction modeled by a short-ranged square-well potential, it has been shown that if the square well is not too short-range, the freezing transition has the character of a first-order phase transition.^{15,16} This first-order freezing transition is also evident in Monte Carlo simulations of Lennard-Jones particles.^{17,18} To the best of our knowledge, no evidence of a first-order collapse transition has been reported in the presence of short-range attractive interactions for flexible chains. However, when there is intrinsic stiffness in the chain, a short-range square-well potential,^{19,20} as well as a Lennard-Jones attraction,¹⁴ will induce a first-order type transition between elongated and compact conformations, confirming early theoretical calculations.²¹

In this paper we investigate, with Monte Carlo simulations, effects of intrinsic chain stiffness on polyelectrolyte condensation. Using a model with explicit Coulomb interactions between polyelectrolyte segments, and in the presence of explicit counterions, we are interested in the fully condensed state as well as in

* Corresponding author. E-mail: m.khan@ms.unimelb.edu.au.

† E-mail: d.chan@unimelb.edu.au.

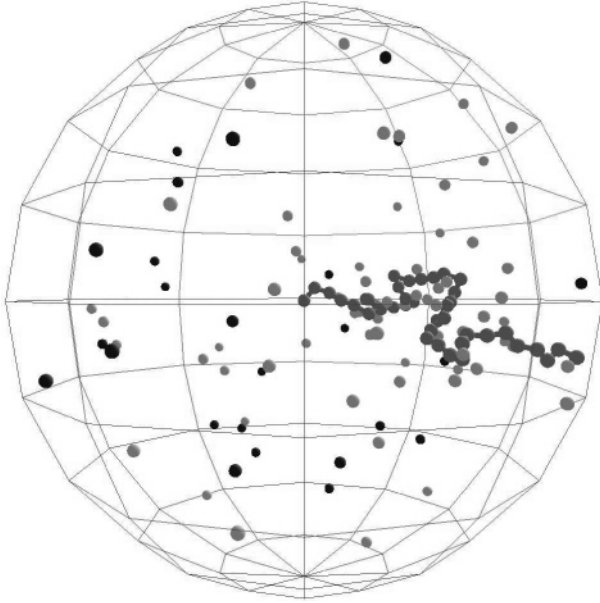


Figure 1. Snapshot from the Monte Carlo simulations showing the model system. The different shades of gray show the polymer, the counterions, and the salt particles. Also shown is the enclosing cell.

intermediate states where the polyelectrolytes are only partially condensed. Furthermore, motivated by single molecule pulling experiments,^{22–25} performed by atomic force microscopy and laser tweezers, we have simulated the response of polyelectrolytes under an external force and thereby have studied the mechanical stability of these chains.

The paper is organized as follows. In section 2 the polyelectrolyte model and the numerical method is introduced. This method is a parallel implementation of the flat histogram technique, which gives directly the free energy and is highly suitable for studying systems close to a phase transition. In section 3, we discuss the effect of adding multivalent counterions to stiff polyelectrolytes. In section 4, force–extension curves are presented and our conclusions are summarized in section 5.

2. The Model and Simulation Methods

2.1. The Cell Model. The system, shown in Figure 1, consists of a single polyelectrolyte which is modeled as a chain of N hard sphere monomers, each with a valence q_m . Each monomer is connected to its neighbors by rigid but freely rotating bonds of fixed length b . The polymer is enclosed in a spherical cell, with radius R_c and one end of the polyelectrolyte is fixed at the center of the cell. Also in the cell are N_c neutralizing hard sphere counterions with a valence q_c . In addition added salt species modeled as hard sphere ions are also present where $N_{s,counter}$ and $q_{s,counter}$ are the number and valence of the salt component with charges of opposite sign to the monomers while $N_{s,co}$ and $q_{s,co}$ are the number and valence of the salt component with charges of the same sign as the monomers. $N_{tot} = N + N_c + N_{s,co} + N_{s,counter}$ is the total number of monomers and ions in the system. All species are confined within the cell and the system obeys the electroneutrality constraint

$$Nq_m + N_cq_c + N_{s,co}q_{s,co} + N_{s,counter}q_{s,counter} = 0 \quad (1)$$

Such a cell model has been used previously to study single polymer properties.²⁶ It is also suitable for extremely dilute solutions where interactions between polymers are small in comparison to intrachain and chain–small ion interactions. For the salt free case the cell size reflects the concentration dependence, while when the amount of added salt is larger than the amount of counterions, the cell size does not influence the single chain conformational properties for dilute systems. All interactions are treated in the so-called primitive model, where the solvent is regarded as a continuum characterized by its dielectric constant ϵ .

The Hamiltonian for the system is

$$U = U_{el} + U_{hc} + U_{angle} + U_{cell} + U_{ext} \quad (2)$$

where the electrostatic term is given by

$$U_{el} = \sum_{i < j}^{N_{tot}} \frac{q_i q_j e^2}{4\pi\epsilon\epsilon_0 |\mathbf{r}_i - \mathbf{r}_j|} \quad (3)$$

and e is the elementary charge. \mathbf{r}_i is the coordinate, and q_i is the valence of particle i . U_{hc} is a hard core potential given by the sum $U_{hc} = \sum_{i < j}^{N_{tot}} u_{ij}^{hc}$ where the pair interaction is

$$u_{ij}^{hc} = \begin{cases} 0, & |\mathbf{r}_i - \mathbf{r}_j| \geq d \\ \infty, & |\mathbf{r}_i - \mathbf{r}_j| < d \end{cases} \quad (4)$$

and d is the hard sphere diameter, taken to be the same for all particles. The stiffness of the polyelectrolyte backbone is modeled by a bond angle dependent potential parametrized in the form

$$U_{angle} = C_{angle} \sum_{i=2}^{N-1} \frac{(\mathbf{r}_{i-1} - \mathbf{r}_i)(\mathbf{r}_{i-1} + \mathbf{r}_i)}{|\mathbf{r}_{i-1} - \mathbf{r}_i| |\mathbf{r}_{i-1} + \mathbf{r}_i|} = C_{angle} \sum_{i=2}^{N-1} \cos(\alpha_i) \quad (5)$$

where α_i is the angle between the two bonds connected to monomer i and C_{angle} is a constant which controls the backbone stiffness of the chain. The term U_{cell} in eq 2 is given by the sum $U_{cell} = \sum_i^{N+N_c} u_i^{cell}$ with

$$u_i^{cell} = \begin{cases} 0, & \mathbf{r}_i \leq R_c \\ \infty, & \mathbf{r}_i > R_c \end{cases} \quad (6)$$

which acts to constrain all species to be within the spherical cell of radius R_c .

To construct force–extension curves, an external force F can be applied at the free end of the polymer which leads to an additional term to the Hamiltonian

$$U_{ext} = -F_{z_N} \quad (7)$$

where z_N is the coordinate of the last monomer in the direction of the applied force. In section 2.3 a more efficient route to obtain force–extension curves is presented. Details concerning simulations of stretched polyelectrolytes is given in previous work.²⁷

In the simulations reported here the following parameters are used: $N = 128$, $R_c = 800 \text{ \AA}$, $d = 4 \text{ \AA}$, $b = 6 \text{ \AA}$, and $\epsilon = 78$. Three different values of the angle constant are used, $C_{angle} = 0, 6$ and 20 , which correspond to persistence lengths $l_p^0 = 12, 39$, and 120 \AA for the

uncharged polymer. For the remainder of this paper, chains with these three values of C_{angle} are labeled as “flexible”, “semi-stiff”, and “stiff” polyelectrolytes. For the chain with $C_{angle} = 0$, the difference between the persistence length (12 Å) and the bond length (6 Å) is due entirely to the hard sphere interaction between the monomers. The monomers of the polyelectrolytes have a valence of $q_m = +1$ and the intrinsic counterions have a valence $q_c = -1$. We also consider the effects of added tetravalent salt by setting $q_{s,co} = +1$ and $q_{s,count} = -4$.

2.2. Monte Carlo Simulations in the Canonical Ensemble. To explore different configurations of the system during canonical Monte Carlo simulations, the small ions are translated as usual while changes in the conformation of the polyelectrolyte backbone are achieved by pivot moves.^{28,29} A pivot move involves choosing a monomer, between 2 and N , and a rotation angle, between 0 and δ_{rot} . The free end of the polymer is then rotated through the chosen angle about the x , y , or z axes. When electrostatic interactions are strong the pivot moves are less likely to be accepted since a large change in energy is associated with such global moves. Therefore, clothed pivot moves³⁰ are employed, in which ions within a distance h from any monomer involved in the pivot are moved with the chain with a probability p_c . The choice of $p_c = 0$ is equivalent to the simple, nonclothed, algorithm while $p_c = 1$ means that all ions within the pivoting portion of the backbone follow the chain. The two parameters h and p_c are input to the simulations and affect the efficiency of the simulation in the same way as the choice of pivot angle parameter δ_{rot} or small ion translation distance parameter δ_{tr} . From our experience and those of others,^{30,31} the choice of h is not sensitive except that h should include the ions closely correlated to the chain. Here we make the empirical choice $h = 3d$. The choice of the probability p_c depends on the strength of the electrostatic interactions. For the case of monovalent counterions in water ($\epsilon = 78$) Gordon and Valleau³⁰ found $p_c = 0.75$ to be optimal, while for trivalent counterions or low dielectric constant ($\epsilon < 20$) $p_c = 1$ is the best choice. For situations between these two extreme cases, p_c is modified accordingly. It is also important to relax the counterions by moving them individually between the clothed global moves. In line with earlier work,^{5,10,32} we choose to perform attempted moves on half of the ions between every global move.

Energies are computed from eq 2, and moves are accepted according to the Metropolis MC scheme.^{33,34} The acceptance probability p_{acc} of a move is modified to incorporate the effects of clothed pivot moves^{30,31}

$$p_{acc} = \min(1, (1 - p_c)^{\Delta m} \exp(-\beta\Delta U)) \quad (8)$$

where $\Delta U = U(\text{new}) - U(\text{old})$ and $\beta = 1/kT$, with k being the Boltzmann constant. $U(\text{new})$ and $U(\text{old})$ are the energies for the new and old configurations. Δm is the difference in the number of ions within the distance h from monomers involved in the pivot move, before and after the clothed move.

The statistics of the end-to-end distance, R_{ee} , of the polyelectrolyte is used as an indicator of convergence of conformational results during simulations. As indicated in the example in Figure 2, convergence is slow for stiff polymers at high added salt concentration where R_{ee} jumps between large and small values as a function of simulation run time. This observation is confirmed

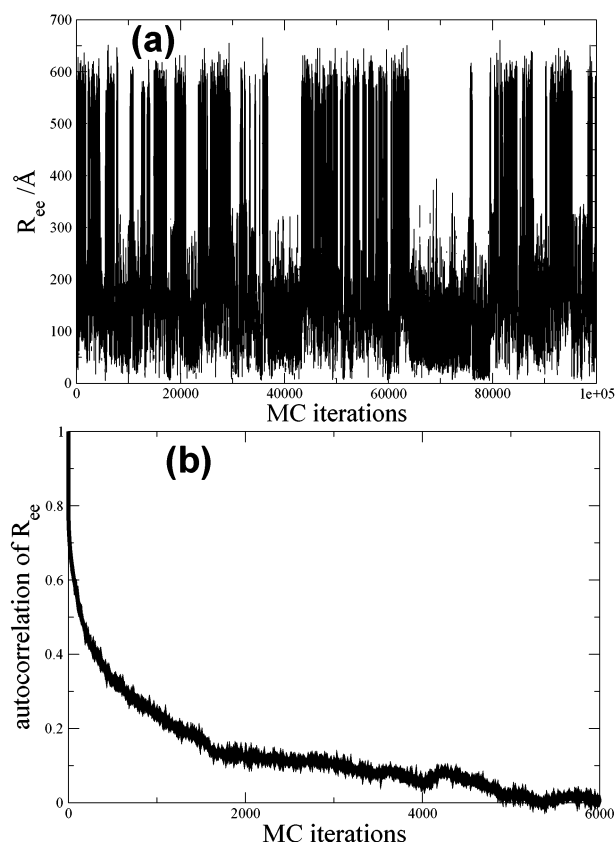


Figure 2. (a) R_{ee} as a function of Monte Carlo iterations for a stiff polyelectrolyte with $l_p^0 = 120$ Å. The polyelectrolyte is neutralized by monovalent counterions and a 4:1 salt is added, corresponding to 1.25 of the polyelectrolyte charge, i.e., 40 tetravalent ions of the opposite sign to the $N = 128$ monomers. Here one iteration is defined as $10 \times N(1 \text{ pivot} + N_{ion}/2 \text{ translations})$, where N_{ion} is the number of small ions. The full simulation of 10^5 iterations took 6 days on a single processor of the Victorian Partnership of Advanced Computing 97 node, 194 CPU Linux Cluster based on Xeon 2.8 GHz CPUs with a Myrinet interconnect. (b) The autocorrelation function extracted from the curve in part a.

by considering the autocorrelation for the end-to-end distance. From Figure 2b, it is clear that only a few independent observations will be found during the full simulation. Since this simulation lasted for 6 days, it is clear that the direct simulation approach presented above is not an efficient way to carry out the simulations for such systems.

2.3. Free Energy Simulations Using Parallel Architecture. It is well-known that simple Monte Carlo does not work well close to phase transitions where the autocorrelation times are very large and therefore the time needed to sample the true statistics of the system becomes prohibitively large. To overcome this problem, a flat histogram method which gives directly the free energy as a function of a specific reaction coordinate is employed.^{35,36} We will use a version of this method that has been shown to be highly suitable for parallel computers.³⁷ The free energy is calculated as a function of R_{ee} , which is also the parameter over which the simulation is parallelized.

The main idea of the free energy algorithm is to modify the MC procedure with a suitable penalty function U^* so that all end-to-end distances will become equally probable. The method used here, introduced by Engkvist and Karlström³⁵ and Wang and Landau,³⁶ resembles umbrella sampling but is different in that the

penalty function is not given as an input to the simulation. Instead, it is generated during the simulation. This penalty function turns out to be related to the free energy or potential of mean force (PMF), $w(R_{ee})$, between the two ends of the chain.^{35,36}

In a normal simulation, a straightforward way of calculating the PMF is to simply calculate the probability of finding the system at a certain end-to-end distance $p(R_{ee})$, and the PMF is related to this probability by

$$w(R_{ee}) = -kT \ln p(R_{ee}) \quad (9)$$

As the probability of visiting high energy states is low, configurations far from the average R_{ee} , namely the extended or compressed configurations, will be sampled infrequently if at all during a simulation. However, by adding an appropriate penalty function U^* to the normal, undisturbed Hamiltonian U it is possible to sample all states of interest. U^* can be derived as follows.

In the canonical ensemble the probability distribution along any reaction coordinate ζ is given by

$$p(\zeta_0) = \frac{\int \exp[-\beta U(\mathbf{r})] \delta[\zeta - \zeta_0] d\mathbf{r}}{\int \exp[-\beta U(\mathbf{r})] d\mathbf{r}} \quad (10)$$

where \mathbf{r} represents all particle coordinates. Adding the penalty function U^* results in a modified probability distribution

$$p^*(\zeta_0) = \frac{\int \exp[-\beta\{U(\mathbf{r}) + U^*(\zeta_0)\}] \delta[\zeta - \zeta_0] d\mathbf{r}}{\int \exp[-\beta\{U(\mathbf{r}) + U^*(\zeta_0)\}] d\mathbf{r}} \quad (11)$$

The original probability distribution can be retrieved from

$$p(\zeta) = C_1 p^*(\zeta) \exp[\beta U^*(\zeta)] \quad (12)$$

where C_1 is a constant. If a simulation is run with a penalty function resulting in a constant $p^*(\zeta)$ this will give

$$p(\zeta) = C_2 \exp[\beta U^*(\zeta)] \quad (13)$$

where C_2 is another constant. Identifying with eq 9, it is clear that

$$U^*(R_{ee}) = -w(R_{ee}) + C_3 \quad (14)$$

where C_3 is a physically unimportant constant additive free energy.

The remaining practical problem is to construct a U^* that will give rise to a uniform distribution of end-to-end distances. The function $U^*(R_{ee})$ is discretized over R_{ee} into equal size intervals. The number of bins used is between 100 and 1000. At the start of the simulation the penalty function U^* is taken to be uniform. Every time the end-to-end distance falls within a particular interval of R_{ee} the corresponding U^* is increased by a certain penalty increment δU^* . This ensures that the distribution function $p^* \sim \exp[-\beta(U + U^*)]$ will approach a constant.

A technical problem is that keeping δU^* constant during the full extent of the simulation will lead to poor statistics. The difference in energy before and after a

MC move will be calculated as $\Delta U + \Delta U^*$. When the distribution function becomes uniform, U^* will start to be updated equally over all R_{ee} , and then fluctuations in ΔU^* will dominate and obscure the information in ΔU . This problem is circumvented by decreasing the penalty increment δU^* as the simulation progresses.^{35,38} In this paper the choice for δU^* is $0.1kT$ to $0.001kT$ at the beginning of the simulation. Following the prescription of Wang and Landau³⁸ the simulation is run until $p^*(R_{ee})$ is "flat", when δU^* is updated according to $\delta U_{new}^* = \delta U^*/2$. "Flat" is defined by all values of $p^*(R_{ee})$ being within δp from the mean $\langle p^*(R_{ee}) \rangle$, where δp is between 0.1 and 0.35 depending on the complexity of the system. When δU^* is updated the histogram containing $p^*(R_{ee})$ is reset to zero and a new histogram is collected for the new value of δU^* . The simulation goes on until δp reaches a predecided value, normally between 10^{-5} and 10^{-8} .

In the parallel implementation of the free energy algorithm, N_{cpu} processors run identical versions of the program but with different initial configurations. Every processor runs independently except that at certain intervals the processor-summed PMF, $\sum_{i=1}^{N_{cpu}} w_i(R_{ee})$, is distributed to all processors. Each processor then continues independently, but with the new global PMF. The idea is that every processor does not have to explore the full PMF as a function of R_{ee} , but together they will do so through sharing the processor-summed PMF.

In the same manner the processor-averaged distribution function

$$\langle p^*(R_{ee}) \rangle_{N_{cpu}} = \frac{1}{N_{cpu}} \sum_{i=1}^{N_{cpu}} p_i^*(R_{ee}) \quad (15)$$

is gathered and this average is checked against the flatness criteria.

To construct force–extension curves using conventional Monte Carlo, an external force has to be applied according to eq 7. Several simulations, each for a different applied force, have to be run to obtain a force–extension curve. However, when using the free energy method described here, the force–extension curve can be found by simply taking the derivative of $w(R_{ee})$ with respect to R_{ee} . The force–extension curve calculated in this manner is equivalent to the strain ensemble, in which one measures the internal retractive force of a chain at fixed elongation. It is possible to convert the results into the stress ensemble, in which one measures the elongation of a chain subjected to a stretching force, but only by recording the connecting information during a simulation.³⁹

For conventional MC, it is possible to estimate statistical errors by collecting independent estimates of expectation values of any physical quantity of interest during the simulation. For flat histogram techniques, this is not applicable since it is only the end product that gives the required function. To quantify the errors of the parallel simulations, we have run some of the simulations 10 times, each with different initial configurations. This approach is used to produce the standard deviations in the results we show.

3. Effects of Adding Multivalent Salt

In this section, we examine the effects of the addition of multivalent salt on the condensation and conformation of polyelectrolytes of varying degrees of polymer

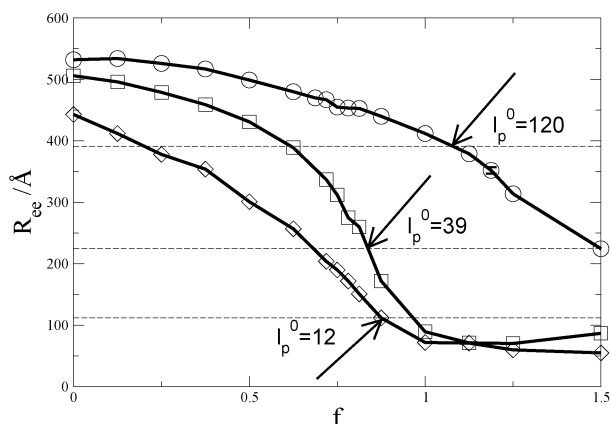


Figure 3. Collapse of polyelectrolytes, neutralized by monovalent counterions, induced by adding a 4:1 salt. The tetravalent ion is oppositely charged to the monomers and f is the proportion of tetravalent ions to monomers, multiplied by 4. The diamonds correspond to a freely jointed chain ($l_p^0 = 12$ Å), the squares to a semi-stiff chain ($l_p^0 = 39$ Å) and the circles to the stiffest chain ($l_p^0 = 120$ Å). The size of a corresponding neutral polymer is given by the dashed line and the point at which the polyelectrolyte has the same average size as the corresponding neutral polymer is indicated by an arrow.

backbone stiffness. We study the effects of a 1:4 electrolyte in which the tetravalent ion is the counterion to the univalent backbone charges on the polyelectrolyte. The added salt concentration is measured in terms of a dimensionless factor f which is the (unsigned) ratio of the total charge from the tetravalent counterions to the total charge on the polyelectrolyte backbone. In the absence of added 1:4 electrolyte, $f = 0$, and the dimensionless added salt concentration $f = 1$ when the total charge from the tetravalent counterions is exactly equal to the charge on the polyelectrolyte backbone.

It is well-known that in an aqueous solvent at room temperatures, the root-mean-squared end-to-end distance, R_{ee} , of a polyelectrolyte with univalent backbone charges and univalent counterions is much larger than that for an uncharged polymer with otherwise the same properties. That is, electrostatic interactions, in the presence of univalent counterions, result in net repulsive intrachain interactions that cause the polyelectrolyte to adopt an expanded configuration compared to the uncharged polymer. For polyelectrolytes of varying stiffness, as characterized by intrinsic nonelectrostatic persistent lengths l_p^0 that vary over a decade from 12 Å to 120 Å, the observed R_{ee} is not sensitive to the chain stiffness. As can be seen from values of R_{ee} at $f = 0$ in Figure 3, a 10-fold difference in the intrinsic nonelectrostatic persistent length only resulted in a difference of about 20% in R_{ee} between the stiffest and the most flexible polyelectrolyte. On the other hand, intrachain electrostatic repulsion increased R_{ee} by a factor of 4 for the most flexible chain with $l_p^0 = 12$ Å but by only 30% for the stiffest chain.

In Figure 3, we see that all three chains, which have different intrinsic stiffness, decrease in size with added multivalent salt (increasing f). For the most flexible chain, R_{ee} decreases almost linearly until it reaches a minimum at about $f = 1$. It has been shown both theoretically⁴⁰ and experimentally⁴¹ that polyelectrolytes assume a minimum size for a certain amount of added salt. When further salt is added, the chain size will actually increase again since high amounts of salt

screen the electrostatic interactions.^{40,41} In previous simulation work of flexible polyelectrolytes,⁴² where the compacting agents were trivalent counterions, the minimum size was found for $1 < f < 3$. The chain sizes increase for $f > 3$, which is well beyond the limits of the present work.

The fact that R_{ee} becomes smaller than that of the neutral polymer for $f > 0.9$, indicates the existence of an effective attractive interaction between the charged monomers at high added salt concentrations. From earlier studies, it is known that the multivalent species are drawn close to the chain and induce an effective monomer–monomer attraction. In contrast, ions of lower valence are found almost homogeneously in the solution.³²

In Figure 3, we also see that the amount of tetravalent ions needed to contract the chain to a certain size increases with the chain stiffness. Furthermore, R_{ee} reaches its minimum at $f = 1$ for the chain with $l_p^0 = 39$ Å, while for the stiffest chain with $l_p^0 = 120$ Å, the minimum is not evident even at the highest concentration of added tetravalent salt examined in this study, $f = 1.5$. The amount of multivalent salt needed to decrease the polyelectrolyte size below that of the neutral polymer is $f = 0.9$ when the intrinsic persistent length is $l_p^0 = 39$ Å and $f = 1.1$ for $l_p^0 = 120$ Å. Similar results have been found in simulations of neutral polymers where compaction was induced by decreasing the temperature.²⁰ For stiffer chains, lower temperatures were needed in order to compact the chains.

The distribution of end-to-end distances shown in Figure 4 provides further insight into the nature of the polyelectrolyte collapse. As multivalent salt is added to the fully flexible chain ($l_p^0 = 12$ Å), the average R_{ee} decreases but the R_{ee} -distribution functions keep the same shape. Without any added multivalent salt, the distribution function for the semi-stiff chain ($l_p^0 = 39$ Å), resembles the distribution function of the flexible chain, except that the curve is centered around a larger R_{ee} . When multivalent salt is added the center of the distribution function moves continuously toward smaller R_{ee} , just as for the flexible chain. However at intermediate concentrations of added salt ($f \sim 0.75$ – 0.90), the distribution function of R_{ee} for the semi-stiff chain broadens to about twice the width as that in the absence of added salt. However, at even higher salt concentrations ($f > 0.90$), the distribution function becomes sharper again.

For the stiff chain ($l_p^0 = 120$ Å), adding small amounts of tetravalent salt ($f \leq 0.8$), does not change the position of the maximum, but results in a tail toward small R_{ee} for the end-to-end distance distribution functions. For larger f , $p(R_{ee})$ has two maxima which indicates the coexistence of an elongated chain and a compact chain. This coexistence seems to remain even for a large amount of added multivalent salt. It is important to point out that the double maxima found in Figure 4c do not directly infer that the two different sized chains coexist within the same solution, but rather that a single chain with a certain electrochemical environment will sample the two configurations according to the figure.

The results in Figure 4 closely resemble those found from multicanonical Monte Carlo simulations of neutral polymer collapse.²⁰ Those simulations show how the internal energy distribution of a flexible polymer has a single maxima which goes to smaller energy values with

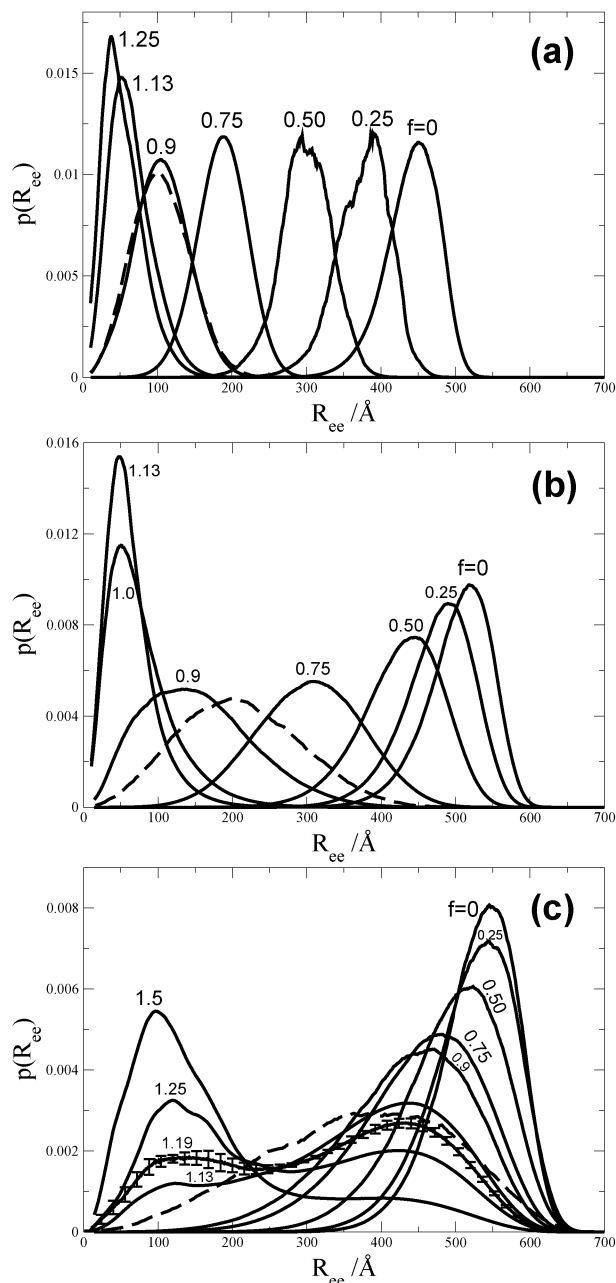


Figure 4. Distribution function of the end-to-end distance for (a) a freely jointed polyelectrolyte ($l_p^0 = 12 \text{ \AA}$), (b) a semi-stiff chain ($l_p^0 = 39 \text{ \AA}$) and (c) a stiff chain ($l_p^0 = 120 \text{ \AA}$). The polyelectrolytes are neutralized by monovalent counterions and a 4:1 salt is added. The numbers labeling the curves indicate the proportion of charges from the tetravalent ions to the charges from the monomers. The dashed lines show the distribution functions for the corresponding uncharged polymers. Note that the y axis of the three graphs have different scales. For the stiff chain, error bars are shown for the $f = 1.19$ case. These error bars are constructed by performing the simulations 10 times.

decreasing energy. Stiff polymers exhibit a double maxima in the energy distribution in much the same way as the end-to-end distributions found in Figure 4c.

There is a certain added salt concentration that will give an end-to-end distribution function that resembles that for the uncharged polymer (dashed curves in Figure 4). That is, as far as the size of the polyelectrolyte is concerned, the charged chain can be made to resemble that of a neutral chain by adding multivalent salt. For the very stiff chain, $l_p^0 = 120 \text{ \AA}$, a second maxima

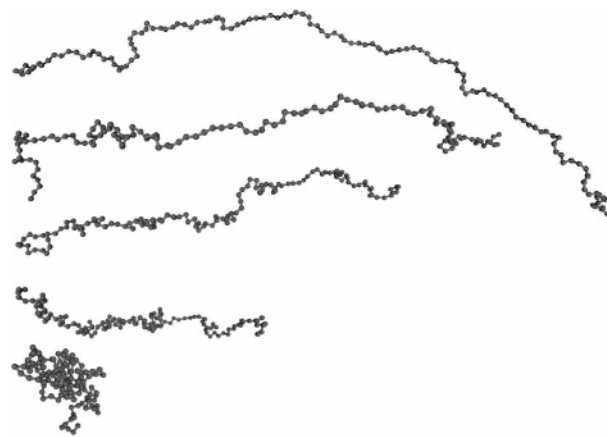


Figure 5. Snapshots from simulations of a freely jointed polyelectrolyte ($l_p^0 = 12 \text{ \AA}$) with $N = 128$ and monovalent counterions which is compacted by adding tetravalent salt. The number of tetravalent salt particles corresponds to, from top to bottom $f = 0.0, 0.25, 0.5, 0.75,$ and 1.0 . Only the polyelectrolyte is shown.

appears which has no counterpart for the neutral polymer.

Even though the size of both stiff polyelectrolytes and freely jointed polyelectrolytes decrease with the addition of multivalent counterions, the chain structure, both at intermediate and high counterions concentration, differ. Snapshots from the MC simulations, shown in Figure 5, illustrates how the freely jointed polyelectrolyte, which is highly extended in the absence of added salt folds locally when multivalent salt is added. At intermediate sizes small compact regions of monomers are found along the stretched backbone. These regions increase in size with added salt, and when the polyelectrolyte is fully neutralized by the multivalent counterions, it collapses into one compact region.

The size of the semi-stiff chain changes rapidly over the added salt concentration ($f \sim 0.65-0.85$). In the presence of a potential that resists local bending, the chain cannot form small compact structures as in the case of the flexible chain. Instead, the polyelectrolyte changes size by bending on a large scale that involved many monomers; see Figure 6.

For the stiff polyelectrolyte, even large scale folding, involving many monomers, is unlikely to occur. The polyelectrolyte remains elongated for salt added up to $f = 1$. For $f \leq 1$, it is possible to find conformations where the whole chain folds at once into a compact structure as reported in simulations of stiff polymers.^{7,14,19,20}

It is a well-known theoretical prediction that the condensed state of stiff polymers and polyelectrolytes are toroids.^{43,44} In the simulations performed here, the only information about the shapes of the compact polyelectrolytes are found from snapshots, as those depicted in Figures 5–7. Our experience, which is supported by earlier simulations of compacted stiff polyelectrolytes^{7,45} as well as stiff neutral polymers,^{13,20,46,47} is that toroidal shapes, rodlike shapes as well as intermediates of the two can be found. In the simulations of polyelectrolytes compacted by tetravalent counterions, reported by Stevens,⁷ the bond angle potential used was $U_{\text{angle}} = k_1(\alpha - \alpha_0)^2 + k_2(\alpha - \alpha_0)^4$, with the equilibrium value $\alpha_0 = 180^\circ$. Stevens found that increasing k_2 , penalising large angle bends, favored toroid structures to rods. Since the cosine potential used here (eq 5) returns lower values than Stevens' angle potential (even when $k_2 = 0$) we would expect a large



Figure 6. Snapshots from simulations of a semi-stiff polyelectrolyte ($l_p^0 = 39 \text{ \AA}$) with $N = 128$ and monovalent counterions which is compacted by adding tetravalent salt. The number of tetravalent salt particles corresponds to, from top to bottom $f = 0.0, 0.25, 0.5, 0.75,$ and 1.0 . Only the polyelectrolyte is shown.

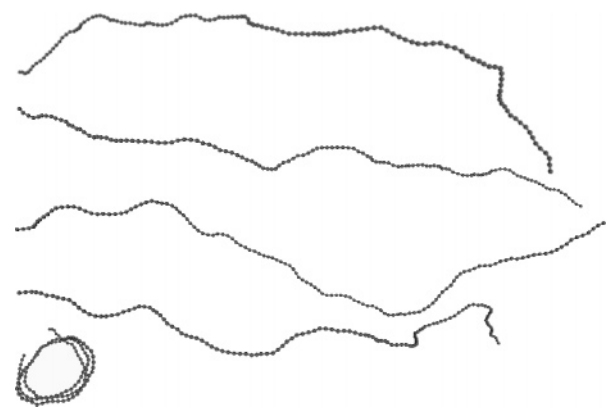


Figure 7. Snapshots from simulations of a stiff polyelectrolyte ($l_p^0 = 120 \text{ \AA}$) with $N = 128$ and monovalent counterions which is compacted by adding tetravalent salt. The number of tetravalent salt particles corresponds to, from top to bottom $f = 0.0, 0.25, 0.5, 0.75,$ and 1.0 . Only the polyelectrolyte is shown. For $f = 1.0$, it is possible to find both compact and elongated conformations.

proportion of rodlike structures. Further investigation is needed to clarify the true equilibrium distribution between these different compact shapes for the cosine angle potential. It is worth noting that simulations where the angle potential $U_{\text{angle}} \sim \cos^2 \alpha$ was used resulted in a mixture of shapes.⁴⁶

4. Force–Extension Curves

Experiments that permit single molecule manipulation have recently been used to extract mechanical information about polymers.^{22–25,48} In these experiments an AFM tip or an optical tweezer is used to extend the polymer and both the length and the applied force are recorded to construct a force–extension curve. This information can readily be constructed with the free energy simulation method used, and results are shown in Figure 8.

In Figure 8a the force–extension curve for a fully flexible polyelectrolyte is shown. It is obvious that even when no external force is present ($F = 0$) the chain

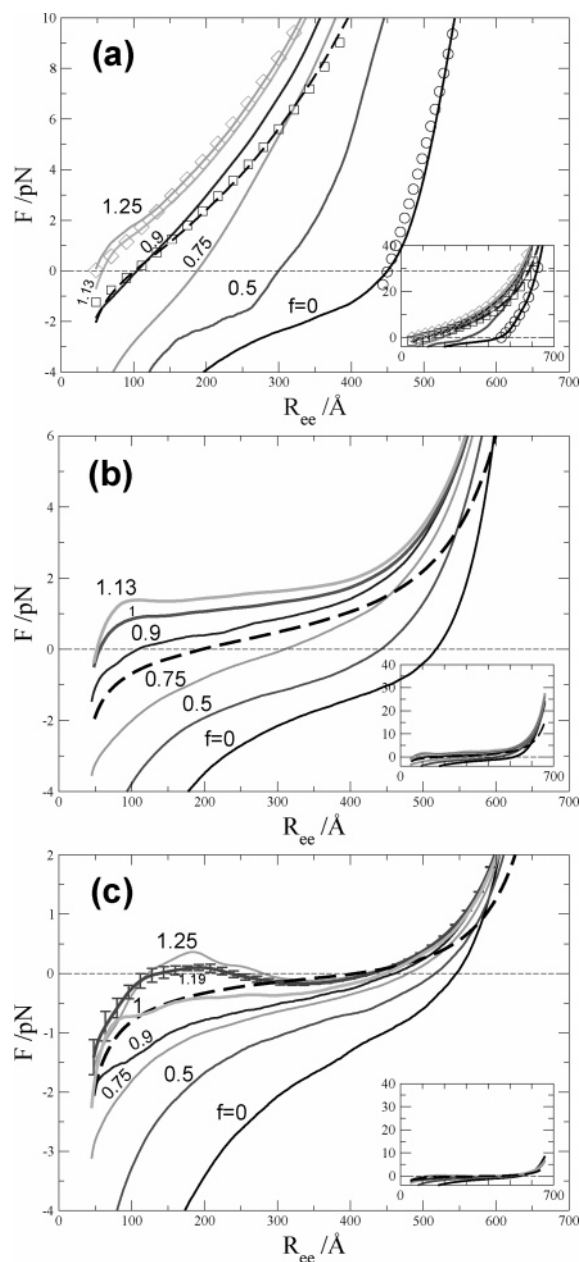


Figure 8. Force–extension curves for (a) a freely jointed polyelectrolyte ($l_p^0 = 12 \text{ \AA}$), (b) a semi-stiff chain ($l_p^0 = 39 \text{ \AA}$), and (c) a stiff chain ($l_p^0 = 120 \text{ \AA}$). The polyelectrolytes are neutralized by monovalent counterions and a 4:1 salt is added. The numbers labeling the curves indicate the proportion of charges from the tetravalent ions to the charges from the monomers. The dashed lines show the force–extension curves for the corresponding uncharged polymers. The symbols in (a) display curves constructed by the interpolation formula given in eq 16. Circles are for the $f = 0$ polyelectrolyte, diamonds for the $f = 1.25$ polyelectrolyte and squares for the uncharged chain. Note that the y axis of the three graphs have different scales. The inserts are zoomed out views of the force–extension curves, and all three have the same scale. For the stiff chain, error bars are shown for the $f = 1.19$ case. These error bars are constructed by performing the simulations 10 times.

without any added multivalent salt ($f = 0$) is in an extended conformation. For the stiffer chains the polyelectrolytes are even more extended and, in fact, most experiments performed on polyelectrolytes with monovalent counterions will only explore the steep rising region for $F > 0$, which is called the finite extensibility region.

With added salt $f > 0$, the flexible chain becomes smaller and the response to an external force is similar to that of a corresponding uncharged polymer.²⁷

The picture for stiffer chains is very different; see Figure 8b. For the semi-stiff chain, the chain size indeed decreases with increasing f as for the flexible chain and when an external force is applied the chain size increases. For small f ($\ll 1$) the chain is already in the finite extensibility region, while if f is large ($f \sim 1$) the force–extension curve shows a plateau of constant F , in which the chain size increases rapidly with small increases in the applied force F .

For the stiff chain the small f behavior is similar to the more flexible chains, while for large f , the plateau region now exhibits two turning points; see Figure 8c. For example, the force–extension curve for the chain with $f = 1.25$, crosses the $F = 0$ line three times, at $R_{ee} = 110, 250$, and 440 Å. The first and the last instances of R_{ee} corresponds to the location of the two maxima found in the size distribution curve in Figure 4, while the middle R_{ee} value corresponds to the minimum in the $p(R_{ee})$ distribution function in Figure 4. The results in Figure 8c demonstrate how a stiff chain with added multivalent salt has two equilibrium sizes, one extended and one compact.

In Figure 8a the force–extension curves computed from our simulations are compared to the corresponding curves for a wormlike chain. In Figure 8, we have used the interpolation formula given by Marko and Siggia⁴⁹

$$\frac{Fl_p}{kT} = \frac{1}{4} \left(1 - \frac{R_{ee} - R_{ee,0}}{(N-1)b} \right)^{-2} - \frac{1}{4} + \frac{R_{ee} - R_{ee,0}}{(N-1)b} \quad (16)$$

where $R_{ee,0}$ is the extension of the chain at zero force. It is clear that the flexible uncharged chain as well as the flexible polyelectrolytes, at all f covered here, can be well described by the WLC model. For the stiffer chains found in Figure 8, parts b and c, the plateaus in the force–extension curves cannot readily be accounted for by eq 16. This kind of deviation from the WLC model, with a pronounced plateau, is a typical feature of force–extension curves produced in stretching experiments of DNA molecules collapsed by multivalent counterions.^{48,50,51}

5. Conclusions

Flexible chains decrease in size to form condensed conformations upon the addition of multivalent salt. The conformations of very stiff chains are unaffected at small amounts of multivalent salt. However at sufficiently high salt concentration the polyelectrolyte collapses by forming toroid-like structures. These observations are also reflected in force–extension curves where a flexible polyelectrolyte gradually increases in size with increasing external applied force, while the force curve for a stiff chain shows a plateau in which the size increases at an almost constant force as the toroidal structure unwinds.

The end-to-end distance distribution functions provides more detailed information on how stiff chains collapse upon the addition of multivalent salt. In Figure 9 the average R_{ee} is drawn together with the most probable end-to-end distances, i.e., the positions of the maximum in $p(R_{ee})$ found in Figure 4c, which is equivalent to where $F = 0$ in the force–extension curves in Figure 8c.

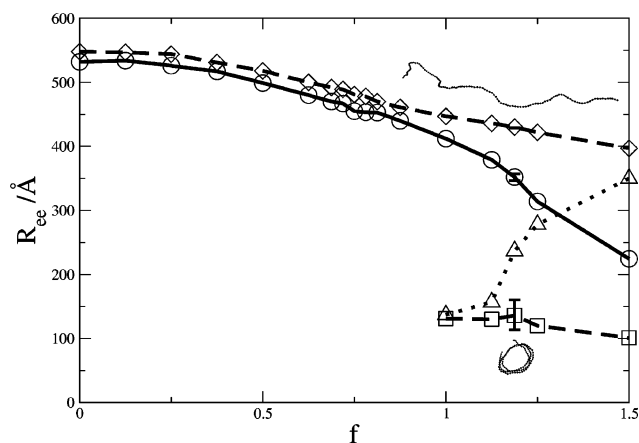


Figure 9. Collapse of a stiff polyelectrolyte ($l_p^0 = 120$ Å), neutralized by monovalent counterions, induced by adding a 4:1 salt. The tetravalent ion is oppositely charged to the monomers and f is the proportion of tetravalent ions to monomers, multiplied by 4. The average end-to-end distance is given by the solid line, while the dashed lines correspond to the most probable collapsed and extended R_{ee} as deduced from the distribution curves in Figure 4c. The dotted line shows the least probable R_{ee} for the polyelectrolyte. Also shown are snapshots of elongated and compact conformations found in the coexistence region.

Figure 9 illustrates clearly how the size of a stiff polyelectrolyte only decreases slightly with added multivalent salts up to $f = 1$. For larger amounts of multivalent salt the stiff chain can take on both compact and elongated conformations. This coexistence has been found experimentally for the stiff polyelectrolyte DNA⁸ and has also been observed in simulations of neutral stiff polymers with short range, solvent induced, monomer–monomer attractions.^{52,19,20}

It is interesting to note that the nature of the coexistence between elongated coils and compact structures found in this study result in the average end-to-end distance decreasing continuously even for stiff chains. That is, even if any single chain is either compact or elongated, the resulting ensemble average is a continuous function of amount of added multivalent salt, a result which supports the similar observations drawn from fluorescence microscopy measurements of DNA condensation.⁸

References and Notes

- (1) Oosawa, F. *Polyelectrolytes*; Marcel Dekker: New York, 1971.
- (2) Ullner, M. Polyelectrolyte models in theory and simulation. In *Handbook of Polyelectrolytes and their Applications*; Tripathy, S., Kumar, J., Halwa, H. S., Eds.; American Science: Los Angeles, CA, 2002.
- (3) Severin, M. *J. Chem. Phys.* **1993**, *99*, 628–633.
- (4) Stevens, M. J.; Kremer, K. *J. Chem. Phys.* **1995**, *103*, 1669–1690.
- (5) Khan, M. O.; Jönsson, B. *Biopolymers* **1999**, *49*, 121–125.
- (6) Winkler, R. G.; Gold, M.; Reineker, P. *Phys. Rev. Lett.* **1998**, *80*, 3731–3734.
- (7) Stevens, M. J. *Biophys. J.* **2001**, *80*, 130–139.
- (8) Yoshikawa, K.; Takahashi, M.; Vasilvskaya, V. V.; Khokhlov, A. R. *Phys. Rev. Lett.* **1996**, *76*, 3029–3031.
- (9) Ueda, M.; Yoshikawa, K. *Phys. Rev. Lett.* **1996**, *77*, 2133–2136.
- (10) Mel'nikov, S. M.; Khan, M. O.; Lindman, B.; Jönsson, B. *J. Am. Chem. Soc.* **1999**, *121*, 1130–1136.
- (11) Zherenkova, L.; Khalatur, P.; Yoshikawa, K. *Macromol. Theory Simul.* **2003**, *12*, 339.
- (12) Ivanov, V. A.; Paul, W.; Binder, K. *J. Chem. Phys.* **1998**, *109*, 5659.
- (13) Kuznetsov, Y. A.; Timoshenko, E. G. *J. Chem. Phys.* **1999**, *111*, 3744.

- (14) Ivanov, V. A.; Stukan, M. R.; Vasilevskaya, V. V.; Paul, W.; Binder, K. *Macromol. Theory Simul.* **2000**, *9*, 488–499.
- (15) Zhou, Y.; Hall, C. K.; Karplus, M. *Phys. Rev. Lett.* **1996**, *77*, 2822–2825.
- (16) Zhou, Y.; Karplus, M.; Wichert, J. M.; Hall, C. K. *J. Chem. Phys.* **1997**, *107*, 10691–10708.
- (17) Liang, H.; Chen, H. *J. Chem. Phys.* **2000**, *113*, 4469–4471.
- (18) Calvo, F.; Doye, J. P. K.; Wales, D. J. *J. Chem. Phys.* **2002**, *116*, 2642–2649.
- (19) Noguchi, H.; Yoshikawa, K. *Chem. Phys. Lett.* **1997**, *278*, 184–188.
- (20) Noguchi, H.; Yoshikawa, K. *J. Chem. Phys.* **1998**, *109*, 5070–5077.
- (21) Grosberg, A. Y.; Khokhlov, A. R. *Statistical Physics of Macromolecules*; AIP Press: New York, 1994.
- (22) Perkins, T. T.; Quake, S. R.; Smith, D. E.; Chu, S. *Science* **1994**, *264*, 822–826.
- (23) Rief, M.; Gautel, M.; Oesterhelt, F.; Fernandez, J. M.; Gaub, H. E. *Science* **1997**, *276*, 1109–1112.
- (24) Mehta, A. D.; Rief, M.; Spudich, J. A.; Smith, D. A.; Simmons, R. M. *Science* **1999**, *283*, 1689–1695.
- (25) Haupt, B. J.; Senden, T. J.; Sevick, E. M. *Langmuir* **2002**, *18*, 2174–2182.
- (26) Wennerström, H.; Jönsson, B.; Linse, P. *J. Chem. Phys.* **1982**, *76*, 4665.
- (27) Khan, M. O.; Chan, D. Y. C. *J. Phys. Chem. B* **2003**, *107*, 8131–8139.
- (28) Lal, M. *Mol. Phys.* **1969**, *17*, 57.
- (29) Madras, N.; Sokal, A. D. *J. Stat. Phys.* **1988**, *50*, 109–186.
- (30) Gordon, H. L.; Valleau, J. P. *Mol. Sim.* **1995**, *14*, 361–379.
- (31) Linse, P.; Lobaskin, V. *J. Chem. Phys.* **2000**, *112*, 3917–3927.
- (32) Khan, M. O.; Mel'nikov, S. M.; Jönsson, B. *Macromolecules* **1999**, *32*, 8836–8840.
- (33) Metropolis, N. A.; Rosenbluth, A. W.; Rosenbluth, M. N.; Teller, A.; Teller, E. *J. Chem. Phys.* **1953**, *21*, 1087–1097.
- (34) Allen, M. P.; Tildesley, D. J. *Computer Simulation of Liquids*; Oxford University Press: Oxford, England, 1989.
- (35) Engkvist, O.; Karlström, G. *Chem. Phys.* **1996**, *213*, 63–76.
- (36) Wang, F.; Landau, D. P. *Phys. Rev. Lett.* **2001**, *86*, 2050–2053.
- (37) Khan, M. O.; Kennedy, G.; Chan, D. Y. C. *J. Comput. Chem.* **2005**, *26*, 72–77.
- (38) Wang, F.; Landau, D. P. *Phys. Rev. E* **2001**, *64*, 056101.
- (39) Inda, M. A.; Frenkel, D. *Macromol. Theory Simul.* **2004**, *13*, 36–43.
- (40) Ha, B.-Y.; Thirumalai, D. *Macromolecules* **2003**, *36*, 9658–9666.
- (41) Volk, N.; Vollmer, D.; Schmidt, M.; Opperman, W.; Huber, K. *Adv. Polym. Sci.* **2004**, *166*, 29–65.
- (42) Sarraguça, J. M. G.; Skepö, M.; Pais, A. A. C. C.; Linse, P. *J. Chem. Phys.* **2003**, *119*, 12621–12628.
- (43) Bloomfield, V. A. *Biopolymers* **1997**, *44*, 269–282.
- (44) Golestanian, R.; Kardar, M.; Liverpool, T. B. *Phys. Rev. Lett.* **1999**, *82*, 4456–4459.
- (45) Sakaue, T. *J. Chem. Phys.* **2004**, *120*, 6299–6305.
- (46) Stukan, M. R.; Ivanov, V. A.; Grosberg, A. Y.; Paul, W.; Binder, K. *J. Chem. Phys.* **2003**, *118*, 3392–3400.
- (47) Montesi, A.; Pasquali, M.; MacKintosh, F. C. *Phys. Rev. E* **2004**, *69*, 021916.
- (48) Baumann, C. G.; Bloomfield, V. A.; Smith, S. B.; Bustamante, C.; Wang, M. D.; Block, S. M. *Biophys. J.* **2000**, *78*, 1965–1978.
- (49) Marko, J. F.; Siggia, E. D. *Macromolecules* **1995**, *28*, 8759–8770.
- (50) Wada, H.; Murayama, Y.; Sano, M. *Phys. Rev. E* **2002**, *66*, 061912.
- (51) Murayama, Y.; Sakamaki, Y.; Sano, M. *Phys. Rev. Lett.* **2003**, *90*, 018102.
- (52) Noguchi, H.; Saito, S.; Kidoaki, S.; Yoshikawa, K. *Chem. Phys. Lett.* **1996**, *261*, 527–533.

MA0491863